The CO_2 molecule as a quantum realization of the 1:1:2 resonant swing–spring with monodromy

R. H. Cushman[1], H. R. Dullin[2], A. Giacobbe[1], D. D. Holm[3,4], M. Joyeux[5], P. Lynch[6], D. A. Sadovskií[7], and B. I. Zhilinskií[7]

[1] *Mathematisch Instituut, Universiteit Utrecht, 3508 TA Utrecht, The Netherlands*
[2] *Mathematical Sciences, University of Loughborough, LE11 3TU Loughborough, UK*
[3] *Mathematics Department, Imperial College London, SW7 2AZ London, UK*
[4] *Theoretical Division, Los Alamos National Laboratory, Los Alamos, NM 87545, USA*
[5] *Laboratoire de Spectrométrie Physique, Université Joseph Fourier, 38402 St. Martin d'Hères, France*
[6] *Met Éireann, Glasnevin Hill, Dublin 9, Ireland*
[7] *Université du Littoral, UMR 8101 du CNRS, 59140 Dunkerque, France*
(Dated: May 5, 2004; Received March 15)

We consider the wide class of systems modeled by an integrable approximation to the three degree of freedom elastic pendulum with 1:1:2 resonance, or the swing-spring. This approximation has monodromy which prohibits existence of global action-angle variables and complicates the dynamics. We study the quantum swing-spring formed by bending and symmetric stretching vibrations of the CO_2 molecule. We uncover quantum monodromy of CO_2 as a nontrivial codimension 2 defect of the three dimensional energy–momentum lattice of its quantum states.

PACS numbers: 45.05.+x, 45.50.-j, 03.65.Sq, 33.20.Vq

The three degree of freedom swing–spring or elastic pendulum [1, 2] can be realized in a vertical gravitational field as an elastic pendulum which can swing in any vertical plane and whose length oscillates spring-wise. Swinging and springing are described in the small oscillation limit by Cartesian displacements (x, y) from the vertical equilibrium $(0, 0)$ and by a small deformation ξ respectively; the momenta conjugate to $q = (x, y, \xi)$ are $p = (p_x, p_y, p_\xi)$. Since this system is invariant under SO(2) rotations in the (x, y) plane, the swing frequencies ω_x and ω_y of the harmonic approximation are equal. The full symmetry group includes time reversal and reflection of the (x, y) plane in any line through its origin.

Our analysis is based on the integrable approximation to the swing-spring. When the swing and the spring frequencies are commensurate, the dynamics in this approximation becomes nontrivial. The case of the 1:1:2 resonance ($\omega_x = \omega_y = \frac{1}{2}\omega_\xi$), named after Fermi in molecular physics, is the most important. It comes up naturally in the study of vibrating linear triatomic molecules where the doubly degenerate bending mode plays the role of the swinging motion and one of the stretching modes is the springing motion. The carbon-dioxide molecule CO_2, which inspired the first comprehensive analysis of the elastic pendulum [1], is a well known textbook example. Remarkably, the swing–spring still has something interesting to offer to the quantum study of the Fermi resonance.

In Ref. [3] additional connections were made between the elastic pendulum and other physical systems of current interest. For example, the modulation equations for the averaged motion of the spring pendulum were transformed into the three complex wave equations (3WE) for *three-wave interactions* that appear in analyzing fluid and plasma systems, and in laser-matter interaction. These 3WE are identical to the Maxwell–Schrödinger envelope equations for the interaction between radiation and a two-level resonant medium in a microwave cavity [4]. The 3WE also govern the envelope dynamics of light-waves in an inhomogeneous material [5, 6]. In certain cases 3WE reduce to Euler's equations for a freely rotating rigid body. Thus, the simple spring pendulum provides a concrete mechanical system which simulates a wide range of physical phenomena.

Many previous studies largely focused on the planar spring pendulum with two degrees of freedom. The three degrees of freedom system exhibits qualitatively new dynamical behavior of stepwise precession of the swing plane [2, 3]. In Ref. [7], this dynamics was shown to be related to *monodromy*, an important topological property of many physical systems [8]. Analysis in terms of the closely related concept of geometric phase was carried out in Ref. [5]. Subsequently, manifestation of monodromy in the quantum Fermi system was uncovered [10]. In this letter we extend our analysis to the concrete CO_2 molecule and explain why and how monodromy becomes the organizing center of the dynamics in systems ranging from atmospheric waves to molecular vibrations.

Analysis based on reduction Reduction is the systematic theory of symmetry and conservation laws in classical mechanics [9]. The action of the spatial symmetry SO(2) on the phase space $\mathbb{R}^6_{q,p}$ is given by the flow of the Hamiltonian vector field of *angular momentum* $L_z = q_x p_y - q_y p_x$. The Fermi resonance assumption implies that the flow of the swing–spring (in the small oscillation limit) is approximately invariant with respect to another S^1 action generated by the flow of

$$N = \tfrac{1}{2}(q_x^2 + p_x^2) + \tfrac{1}{2}(q_y^2 + p_y^2) + (q_\xi^2 + p_\xi^2),$$

which is the principal part of the Hamiltonian of the linearized system. In other words, our system has a nontrivial approximate *dynamical symmetry* S^1. Note that $\{L_z, N\} = 0$ and the actions of SO(2) and S^1 commute. Since the S^1 symmetry is approximate we should first *normalize* our initial Hamiltonian with respect to it. The resulting normal form $H(q, p)$ Poisson commutes both with N and L_z, and gives the particular integrable approximation which we analyze further.

Singular reduction of the SO(2) $\times\, S^1$ symmetry [7, 10] is at the heart of our analysis. Like any SO(2) $\times\, S^1$ invariant polynomial in (q, p) the normal form H can be expressed as a polynomial in (N, L_z) and

$$\begin{aligned} R =& \tfrac{1}{2}(q_x^2 + p_x^2 + q_y^2 + p_y^2), \\ S_\pm =& \tfrac{1}{4}\left[z_\xi(\bar z_x^2 + \bar z_y^2) \pm \bar z_\xi(z_x^2 + z_y^2)\right], \quad z = q + \mathrm{i}p, \end{aligned}$$

where $S = S_+$ is the principal *Fermi interaction term*. The discrete symmetries further simplify H so that it does not depend on S_- and has only even powers of L_z.

The *reduced* Hamiltonian is a polynomial $H_{n,\ell_z^2}(R, S)$ obtained from H by fixing the values of the first integrals N and L_z to $n \geq 0$ and $-n \leq \ell_z \leq n$, respectively, and treating them as parameters. After neglecting constant terms $c(n, \ell_z^2)$ and rescaling, the leading terms in H_{n,ℓ_z^2} near the exact resonance limit can be written as the *Fermi model Hamiltonian* $\mathcal{H}_\lambda = S + \lambda R$. Here $\lambda \ll 1$ represents a detuning of the resonance. Note that $\lambda = 0$ for the swing–spring and the three-wave equation. These systems are described in first approximation by the Fermi interaction term.

The complete overview of all possible motions of the swing–spring is given by the energy–momentum map

$$\mathcal{EM} : \mathbb{R}^6 \to \mathbb{R}^3 : (q, p) \to \big(L_z(q, p), H(q, p), N(q, p)\big)$$

whose fibers are the combined level sets of the three constants of motion, the momenta (N, L_z) and energy H. In the space $\mathbb{R}^3_{\ell_z,h,n}$ the image of $\mathcal{EM}$ (Fig. 1) is a filled cone C with vertex at the point $(0, 0, 0)$. Each constant $n > 0$ slice of C is an eye-shaped closed disk with two singular points at the boundary and one isolated singular point inside. This latter singularity is part of an isolated *singular thread* inside C. Note that C is symmetric with respect to $\ell_z \to -\ell_z$ and $h \to -h$ due to time-reversal symmetry and the pseudo-symmetry $(\xi, p_\xi) \to (-\xi, -p_\xi)$ which changes the sign of $\mathcal{H} = S$.

As illustrated in Fig. 1, regular values (ℓ_z, h, n) (shaded area) lift to 3-tori in $\mathbb{R}^6_{q,p}$, while values on the boundary of C lift to relative equilibria $\mathbb{S}^1$ or $\mathbb{T}^2$. Every singular value on the thread $(0, 0, n)$, $n > 0$, lifts to a singular 3D variety $\mathfrak{T}_n$ which has one singular circle $\mathbb{S}^1$. This circle is the pure springing unstable relative equilibrium and is a special short period orbit of the S^1 action. The regular part of $\mathfrak{T}_n$ is the separatrix of this periodic orbit.

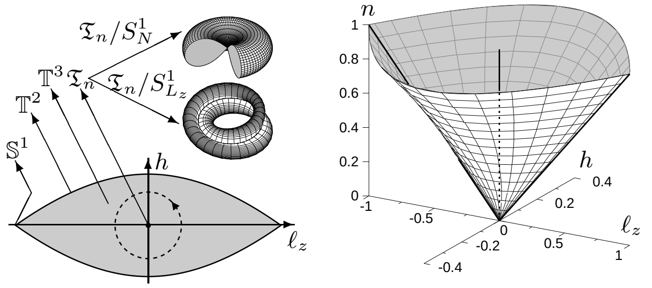

FIG. 1: Range of the $\mathcal{EM}$ map of the Fermi model system with Hamiltonian $\mathcal{H} = S$ (right), its constant $n > 0$ section (left bottom) where the dashed line represents the path Γ used in computing monodromy, and fibers (left top)

The $\mathcal{EM}$ map of the more general Fermi model system with $\lambda \neq 0$ is qualitatively the same for all $n \gg \lambda$ and can be obtained by a small continuous deformation of the $\lambda = 0$ case. The only difference when $n \gg \lambda \neq 0$ is that there is no pseudo-symmetry $h \to -h$.

The presence of the one parameter family of singular fibers $\mathfrak{T}_n$ is the topological reason for all of the nontrivial dynamics and is also the origin of *monodromy*, or the obstruction to global action–angle variables [8]. Our system has two global actions L_z and N, which define respective periodic flows on all regular tori $\mathbb{T}^3_{\ell_z,h,n}$. On the other hand $\mathcal{H}$ is not an action because its flow is not periodic. In a sufficiently small neighborhood $D_{\ell_z,h,n}$ of a given $\mathbb{T}^3_{\ell_z,h,n}$ we can always define a *local third action integral* $I = I(L_z, N, H)$ as a smooth single-valued Hamiltonian function of (q, p) whose flow is periodic on all regular tori in $D_{\ell_z,h,n}$. But we cannot extend I to be defined on all of phase space. In particular I fails to be continuous on $D_\Gamma \subset \mathbb{R}^6_{q,p}$ where Γ is any closed path which encircles the singular thread in the domain of regular $\mathcal{EM}$ values, i.e., the regular $\mathbb{T}^3$ torus bundle over Γ is nontrivial.

The plane switching phenomenon Starting with a weakly unstable vertical springing, the swing–spring evolves into an almost planar swinging. This latter is transient and the system returns to its original springing motion, as one would expect. When this cycle repeats we realize that swinging and springing are very intricately intertwined [2, 3, 7]: the azimuth of the swing plane changes from one swinging phase to the next by an amount $\Delta\vartheta$ which is extremely sensitive to the initial conditions even for very small nonzero amplitudes.

The small oscillation frequencies of the swing–spring are in the 1:1:2 resonance when the spring force constant k, the mass m, and the unstretched length l_0 are chosen so that $3mg = kl_0$ [10]; the reduced Hamiltonian is

$$H_{n,\ell_z} = c\,n + \tfrac{3}{16}\,c^{3/2}\,S, \quad c = \sqrt{k^3/(g^4 m^5)}.$$

The reduced dynamics [7] is governed by the equation for the reduced spring energy a, namely

$$\ddot{a} = -\mu^2 \frac{\mathrm{d}}{\mathrm{d}a}\left[2a\,(2n - 2\ell_z - a)\,(2n + 2\ell_z + a)\right], \qquad (1)$$

where $\mu = 3\sqrt{2}/16$. The special solution for $\ell_z = 0$ and $a = 2n$ corresponds to the pure springing periodic orbit.

The stepwise advance of the swing plane

$$\Delta\vartheta = \oint \dot{\vartheta}\,\frac{\mathrm{d}t}{\mathrm{d}a}\,\mathrm{d}a, \qquad (2)$$

where

$$\dot{\vartheta} = 2\ell_z\,(h - 2n)\left[(2n - 2\ell_z - a)(2n + 2\ell_z - a)\right]^{-1},$$

is smooth on the set of regular $\mathcal{EM}$ values (ℓ_z, n, h), but is *not single valued*. Indeed, carefully expanding the integral (2) near the critical line $\ell_z = 0$ gives

$$\Delta\vartheta = -\arg\zeta + n^{-1}\mathrm{O}(|\zeta|), \quad \zeta = (h - n)\mu^{-1}n^{-\frac{1}{2}} + \mathrm{i}\ell_z.$$

This multivaluedness of $\Delta\vartheta$ explains why it is so sensitive to the initial conditions near $\ell_z = 0$. In fact $\Delta\vartheta$ cannot be defined continuously along the path Γ discussed above (see Fig. 1) because its value jumps by 2π. This is a direct manifestation of monodromy.

The CO_2 molecule The CO_2 molecule has six internal degrees of freedom. The symmetric stretching ν_1 and the doubly degenerate bending ν_2 are in a very strong Fermi resonance. In order to focus on the (ν_1, ν_2) subsystem we average rotations and the asymmetric stretch vibration ν_3 in the complete Hamiltonian [11, 12] with the vibrational potential determined in Ref. [13] from spectroscopic data. Then we normalize with regard to the dynamical Fermi symmetry and obtain the reduced effective Hamiltonian

$$\begin{aligned} H_{n,\ell_z,v,j} &= -2531.745 + 676.757n + 2396.202v \\ -12.5294v^2 &- 9.7575nv - 0.7203n^2 - 1.4972\ell_z^2 + \dots \\ +0.39161j^2 &- R\,(3.8182 + 2.6194v + 1.4136n + \dots) \\ &+ S\,(37.0510 - 0.1967n - 0.2253v + \dots) \\ &+ R^2\,(3.8711 + \dots) - RS\,(0.3055 + \dots) + \dots \end{aligned}$$

Here j is the amplitude of the total angular momentum and v is the action of the ν_3 oscillations. The coefficients are in cm^{-1}. We consider small $v \ll n$ and $j \ll 10^2$.

In order to analyze the quantum manifestations of classical monodromy in the CO_2 molecule, we construct the *quantum $\mathcal{EM}$ lattice* whose points represent eigenstates of $H = H_{n,\ell_z,v,j}$, see Fig. 2. This analogue of the classical $\mathcal{EM}$ map is the joint spectrum of three commuting operators H, L_z, and N corresponding to the constants of motion of the classical integrable approximation.

The eigenvalues of the quantum analogues of the global actions N and L_z equal $\hbar$ times respective global integer quantum numbers n_N and $n_{L_z} = \pm n_N, \pm n_N \mp 2, \dots,$

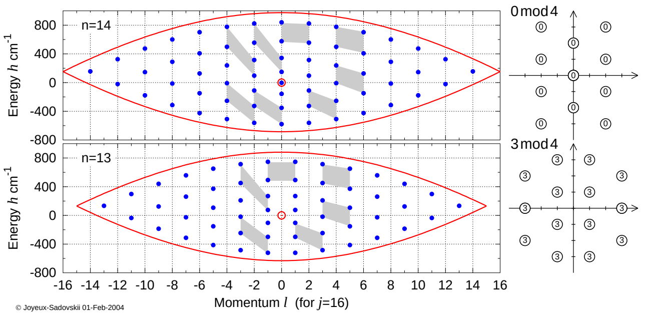

FIG. 2: Constant n_N polyad sections of the $\mathcal{EM}$ lattice of the quantum states of CO_2 (dots) with $j = 16$ and $v = 0$ and the boundary of the image of the classical $\mathcal{EM}$ map (lines); the $\mathcal{EM}$ lattices of the Fermi model Hamiltonian $\mathcal{H} = S$ near the classical singular value $\ell_z = h = 0$ (right). The difference between computed and observed quantum energies is negligible in the scale of the figure.

where n_N labels large manifolds of states called *vibrational polyads*, and n_{L_z} selects multiplets in the internal structure of polyads. Note that the $n_{L_z} \to -n_{L_z}$ symmetry of the $\mathcal{EM}$ lattice is due to the time-reversal invariance of the system. By the usual correspondence principle the classical values (n, ℓ_z) equal $(n_N + 2, n_{L_z})$. Each polyad has $\frac{1}{4}(n_N + 2)^2 - \kappa$ states with $\kappa = 0$ or $\frac{1}{4}$ for even or odd n_N respectively; the number of states in each (n_N, n_{L_z}) multiplet equals $\frac{1}{2}(n_N - |n_{L_z}|) + 1$.

Like the local classical action I, we can define the third quantum number n_I and enumerate the eigenvalues $\langle H \rangle$ for states with fixed (n_{L_z}, n_N). Due to quantum monodromy n_I can only be defined *locally*. The whole lattice has a *defect* which prevents global definition of n_I. We can see this from the *elementary cell diagram* in Fig. 2, top, where cells are shown as small shaded quadrangles. Each cell represents locally chosen I and corresponding n_I. Using the basis vectors of the current cell we can extend it uniquely to adjacent cells. However, when we make a tour along Γ, we come back to a *different* cell and therefore n_I has changed.

The above demonstration of monodromy for one polyad cannot characterize the three-dimensional (3D) $\mathcal{EM}$ lattice because individual polyad slices have different patterns. This lattice has a nontrivial codimension 2 ray defect which corresponds to the singularity of the classical system. We should follow simultaneously two 2D-cells which belong to different polyads and make up the ceiling and the floor of one 3D-cell. In order to simplify our task we can show that for sufficiently large $n_N \geq 1$ the CO_2 lattice near the defect can be continuously deformed into that of the Fermi model with Hamiltonian $\mathcal{H} = S$ (Fig. 2, right). Since such deformation preserves all topological properties, we can study monodromy using the simpler model lattice [10].

Defect of the model $\mathcal{EM}$ lattice The idea of using integer quantum numbers to represent quantum states completely goes back to the foundations of quantum mechanics. In our context it means mapping the $\mathcal{EM}$ lattice into a regular simple cubic lattice $\mathbb{Z}^3$. (Back in the classical system this corresponds to replacing the $\mathcal{EM}$ map for a momentum map with three global actions.) We already know that monodromy makes this globally impossible. What we can do is to make an *atlas* of semi-global $\mathbb{Z}^3$ charts on the whole $\mathcal{EM}$ lattice and specify how the lattice changes going from one chart to another. The whole $\mathcal{EM}$ lattice becomes a $\mathbb{Z}^3$ lattice with *defects* [14] that are further characterized by computing monodromy.

The $\mathcal{EM}$ lattice of the $\mathcal{H} = S$ Fermi model has the defect ray $\{n_{L_z}{=}\langle\mathcal{H}\rangle = 0,\, n_N > 0\}$. Knowing the number $\mathcal{N}(n_N, n_{L_z})$ of states in polyads and multiplets, and using the $\langle S\rangle \to -\langle S\rangle$ pseudo-symmetry we find that the polyad sections near $n_{L_z} = \langle S\rangle = 0$ have four qualitatively different patterns depending on $n_N \bmod 4$ [10], two of which are shown in Fig. 2, right. In order to regularize such lattice while retaining its symmetries we need an atlas of four charts A, B, C, D shown in Fig. 3. The charts can be considered as pieces of the same $\mathbb{Z}^3$ lattice, some parts of which have been cut out. The boundaries of the charts (cuts) are readily identified along the directions of this ambient $\mathbb{Z}^3$ lattice. Thus, to reproduce

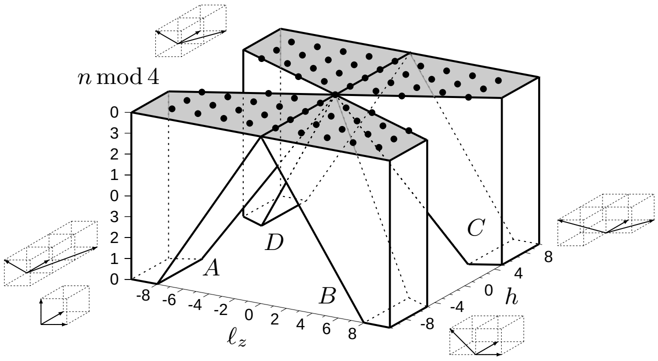

FIG. 3: Three-dimensional model of the regularized quantum $\mathcal{EM}$ lattice of the quantum 1:1:2 resonant swing–spring.

the central part of the eye-shaped $0 \bmod 4$ slice in Fig. 2, we take the top slice of the lattice in Fig. 3 and glue the boundaries of its two cuts together while keeping ℓ_z constant. Glueing the three wedge cuts of the full lattice in Fig. 3 leads to two defects: one which we seek to describe and the other which goes along the "rooftop" in Fig. 3 and can be moved away to arbitrarily large n_N.

Clearly the elementry cell moves unchanged within any $\mathbb{Z}^3$ chart in our atlas. So all we have to do is to determine how the cell changes when we "cross the cuts" or change charts. It turns out that the total transformation matrix M is a product of $3{\times}3$ matrices in $\mathrm{SL}(3,\mathbb{Z})$ each corresponding to one cut and depending on the geometry of the cut and the direction in which it is crossed [10]. Thus starting with a cubic unitary cell in map A and going counterclockwise $A \to B \to C \to D \to A$ along the path Γ in Fig. 1 we obtain $M = M_{DA}M_{CD}M_{BC}M_{AB}$ where the contribution of each cut can be found straightforwardly by traversing it with a unit cell. For any particular cell defined by matrix $K \in \mathrm{SL}(3,\mathbb{Z})$ with respect to the cubic lattice A the transformation is $K^{-1}MK$. It can be shown that M belongs to the same conjugacy class in $\mathrm{SL}(3,\mathbb{Z})$ as $\left(\begin{smallmatrix}1&0&0\\1&1&0\\0&0&1\end{smallmatrix}\right)$. So in this sense we have a trivial extension of the $\left(\begin{smallmatrix}1&0\\1&1\end{smallmatrix}\right)$ monodromy known in a number of systems with two degrees of freedom [8].

Discussion As modern physical theories tend to embrace concisely all the concrete and detailed information on the systems provided by classical and quantum mechanics, our work shows most convincingly that such global description should rely on the singularities of the classical integrable approximation as its organizing center. We have analyzed the singularity of the Fermi system and its molecular quantum realization. This system has monodromy whose 3×3 matrix is nontrivial in the natural coordinates. Our regularized quantum $\mathcal{EM}$ lattice with elementary defects gives a new technique (i) to classify typical local patterns of joint quantum spectra near the defects, (ii) to analyze the global arrangement of quantum numbers, and (iii) to study more complicated obstructions and defects as well as their role in the transition to chaos. It is now tempting to think of experimental quantum dynamical manifestations of monodromy.

We acknowledge the support by the EU network MASIE, Contract No. HPRN-CT-2000-00113.

[1] A. Vitt and G. Gorelik, Zh. Tekhn. Fiz. **3**, 294 (1933).
[2] P. Lynch, Intl. J. Nonlin. Mech. **37**, 345 (2002); P. Lynch and C. Houghton, Physica D **190**, 38 (2004).
[3] D. D. Holm and P. Lynch, SIAM J. Applied Dyn. Syst. **1**, 44 (2002).
[4] D. D. Holm and G. Kovačič, Phys. D **56**, 270 (1992).
[5] M. S. Alber, G. G. Luther, J. E. Marsden, and J. M. Robbins, Phys. D **123**, 271 (1998).
[6] D. David and D. D. Holm, J. Nonlinear Sci. **2**, 241 (1992).
[7] H. Dullin, A. Giacobbe, and R. H. Cushman, Physica D **190**, 15 (2004).
[8] J. J. Duistermaat, Commun. Pure Appl. Math. **33**, 687 (1980); For recent references on atomic and molecular systems with monodromy see K. Efstathiou, M. Joyeux, and D. A. Sadovskií, Phys. Rev. A **69**, 032504 (2004).
[9] R. H. Cushman and L. Bates, *Global aspects of classical integrable systems*, (Birkhauser, Basel, 1997).
[10] A. Giacobbe, R. H. Cushman, D. A. Sadovskií, and B. I. Zhilinskií, in preparation.
[11] E. B. Wilson, J. C. Decius, and P. C. Cross, *Molecular vibrations* (McGraw-Hill, New-York, 1955).
[12] J. K. G. Watson, Mol. Phys. **19**, 465 (1970).
[13] J. Zuniga, A. Bastida, M. Alacid, and A. Requena, J. Mol. Spectrosc. **205**, 62 (2001).
[14] B. I. Zhilinskií, arXiv:quant-ph/0303181